Investigation of Extracting a Transfer Function from Transient Signals During Switching Operations of Inverters for On-Line Monitoring of Electrical Machines

1st Hujun Peng
Institute of Electrical Machines (IEM)
RWTH Aachen University
Aachen, Germany
hujun.peng@iem.rwth-aachen.de

2nd Yue Yu
Institute of Electrical Machines (IEM)
RWTH Aachen University
Aachen, Germany
yue.yu@iem.rwth-aachen.de

3rd Simon Steentjes
Institute of Electrical Machines (IEM)
RWTH Aachen University
Aachen, Germany
simon.steentjes@iem.rwth-aachen.de

2025 IEEE Workshop on Electrical Machines Design, Control and Diagnosis (WEMDCD) | 979-8-3315-2074-8/25/$31.00 ©2025 IEEE | DOI: 10.1109/WEMDCD61816.2025.11014160

***Abstract*—This paper investigates the potential of using electric terminal signals of induction machines for online fault monitoring through experimental studies. The results reveal that by analyzing the transient voltage signals at electrical machine terminals, including the neutral point, it is possible to detect inter-turn short-circuit electrical faults online in real-time. The detection mechanism is based on analyzing signals and their correlation in high-frequency domains. These transient signals naturally exist due to the inverter-fed operations. Therefore, this work invokes the potential of realizing a non-invasive and convenient online monitoring of insulation fault detection.**

***Index Terms*—Electric Machine, Inter-turn Short Circuit, Insulation Fault, Real-Time Condition Monitoring, Transient Signal Analysis**

I. Introduction

As industrialization and the electrification of heavy industries accelerate globally, the widespread deployment of large electric motors and generators in sectors such as energy, mining, and manufacturing has become increasingly prevalent. Ensuring these large machines' operational efficiency, safety, and reliability poses a formidable challenge to the industry. Recent advances have seen the development of online condition monitoring systems based on computationally inexpensive digital twin (DT) technology [1], aiming to facilitate predictive maintenance, thereby reducing the levelized production costs and enhancing the lifespan of industrial equipment [2]. Condition Monitoring Systems (CMS), such as *SIPLUS CMS1200* [3] from Siemens AG and *CMSadvanced* [4] from the company Bachmann, face unresolved issues that compromise their effectiveness. For example, they mainly focus on mechanical faults using vibration signals and cannot treat the most challenging electrical fault, the inter-turn short circuit (ITSC). Research indicates that electrical insulation in stator and rotor windings is a critical point of failure in machines [5], with over 45 % of electrical machine failures attributed to faults in these components, primarily due to insulation breakdowns leading to internal short circuits [6]. If not addressed timely, these faults can exacerbate issues such as increased excitation current, reduced reactive power output, or mechanical failures like torque ripple during turbine operations [7], [8]. Current large machine monitoring systems are primarily based on ISO-18436 standards, which utilize vibration analysis, temperature measurements, and oil analysis. These methods predominantly focus on mechanical, thermal, and chemical signals but often neglect the crucial analysis of electrical signals. Despite the availability of alternative approaches like online partial discharge testing for electrical machines, these methods still face significant drawbacks, such as susceptibility to noise interference and high technical costs. Consequently, there is a pressing need within the industry for a sensitive and robust method to facilitate the online, in-service detection of internal short-circuit faults in motors [9]–[11].

In recent years, the high-frequency modeling technology of electric machines has been developed, which is based on the impedance spectrum of electrical machines to model their transient response behavior. These models are advantageous due to their low computational demand and ability to accurately predict transient signals in machines [12]–[14]. After being validated across various electric machine types, high-frequency modeling serves as a technical foundation for enabling the online identification of inter-turn winding short-circuit faults in large electric machines based on transient signals at the machine terminals. Based on existing technology, several studies attempt to extract information related to internal structure and insulation properties by analyzing the frequency response behavior of components. Research [15] developed a high-frequency model for locating faults within cables, but this model heavily relies on accurate and comprehensive material parameters. Research [16] proposed a method for identifying internal short-circuit faults using Sweep Frequency Response Analysis (SFRA). However, SFRA is highly susceptible to environmental influences and is time-consuming, hindering its real-time fault diagnostics application. Research [17] analyzed the impact of changes in parasitic capacitance within the winding on the terminal frequency response behavior. However, the influence of the conductors' inductances and resistances is not considered. So far, there is no method using the transmittance spectrum between machine terminal and neutral point voltage signals for detecting ITSC, which will be treated here. In other words, this paper will explore the feasibility of this identification method through experimental analysis using a small-scale Doubly Fed Induction Machine (DFIM). Due to limitations in our prototype, where the rotor's neutral point is inaccessible, transient voltage signals are injected into the stator winding instead of the rotor winding. Nonetheless, the fundamental principles remain applicable across all winding types when they are excited by PWM-form voltage signals. In actual machine operation, PWM voltage pulses generated by inverters are not entirely filtered at the machine terminals. These pulses can transfer to the neutral point [18], which fulfills the precondition of using our method developed in this paper. The organization of this work is as follows: Section II is devoted to describing experiments with time-domain impedance measurement and related inferences. Section III validates these inferences through measurements in the time domain on a test bench. Section IV presents conclusions and an outlook on future research directions.

II. Experiment Setup and Impedance Measurement with Different Short-Circuit Degrees within One Phase

Previous research has shown that common-mode impedance reflects changes in the parasitic capacitance of the insulation layer in stator windings [19], [20]. Therefore, the common-mode impedance of the DFIM stator winding is primarily measured with the impedance analyzer 'E4990A' of the company Keysight, offering a 20 Hz to 120 MHz range, 0.045 % resolution, and a $25\,\text{m}\Omega$ to $40\,\text{M}\Omega$ measurement range [21]. Figures 1 and 2 illustrate the measurement setup. In order to minimize the impact of the rotor on the measurement, the three phases of the rotor winding are short-circuited. The common-mode impedance spectrum of the machine is measured from 100 Hz to 10 MHz, displaying a phase angle of -90° at lower frequencies and gradually exhibiting inductive behavior as the frequency increases, forming resonance points in the spectrum.

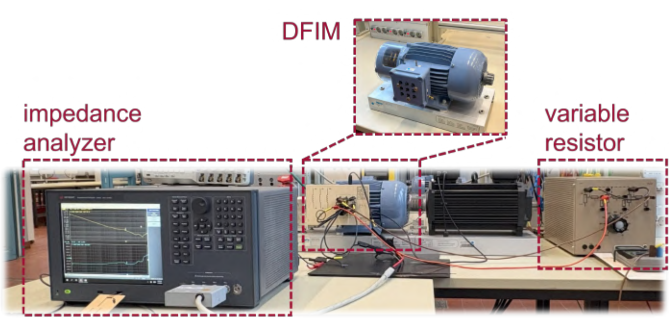

Fig. 1. Measurement of the common-mode impedance of the DFIM stator winding with different short-circuit resistance between the U phase terminal and neutral point.

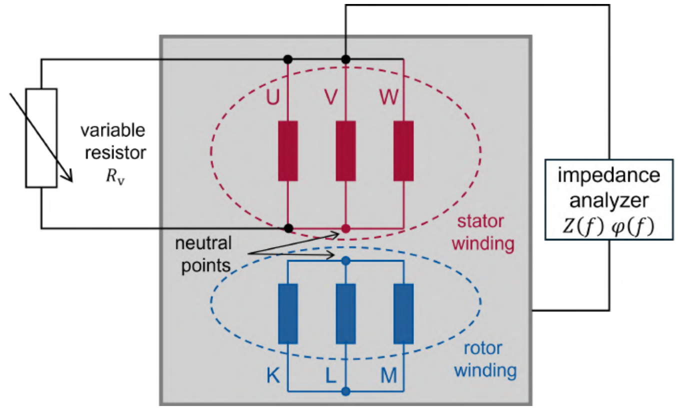

Fig. 2. Sketch of impedance measurement of common mode impedance with variable resistance for short-circuiting U phase winding.

Following the approach described in [22], a variable resistor is connected in parallel between the U-phase terminal and the neutral point to simulate inter-turn short circuits within a single phase during machine operation, as illustrated in Fig. 2. It has to be mentioned that the parallel short-circuited resistance is merely three times larger than the original stator phase winding resistance. The resistance value simulates different locations of internal short-circuit faults. When a short circuit occurs between two adjacent turns within the same phase, it is approximated by paralleling a high-resistance resistor between the U and the neutral point. As the variable resistor increases, the severity of the short circuit within one phase decreases.

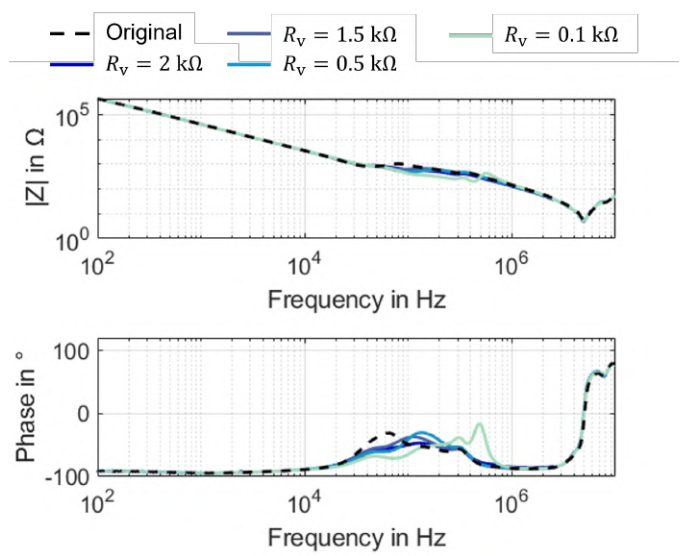

Fig. 3. Measured common-mode impedance spectrum between UVW and housing at various values of parallel resistors R_v for short-circuiting U phase winding.

Fig. 3 illustrates the measured common-mode impedance spectrum of the DFIM stator winding with various values of parallel resistors R_v, specifically $2\,\text{k}\Omega$, $1.5\,\text{k}\Omega$, $0.5\,\text{k}\Omega$, and $0.1\,\text{k}\Omega$. These cases are labeled as Short-circuit Conditions (SC) 'case 1', 'case 2', 'case 3', and 'case 4', respectively, with

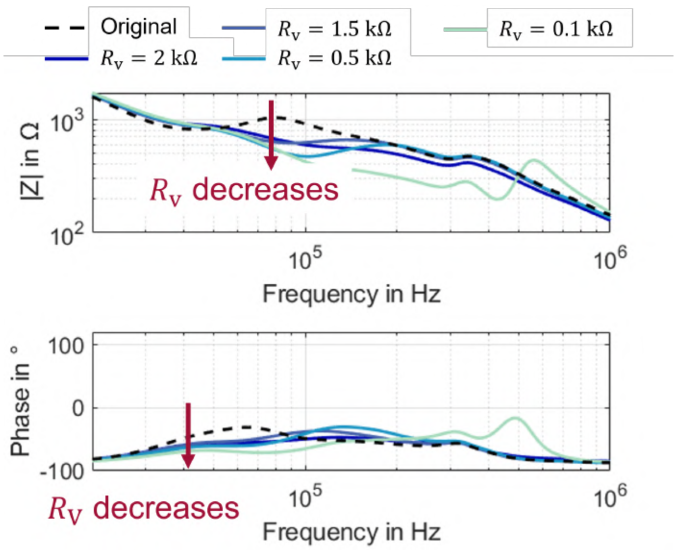

Fig. 4. Zoomed view of measured common-mode impedance spectrum between UVW and housing at various values of parallel resistors R_v for short-circuiting U phase winding.

larger numbers indicating more extraordinary coil turns affected by the short circuit. Compared to the parallel resistance used in [22], the parallel resistance that will be introduced will be several hundred times larger than the stator winding resistance of DFIM and will be much more challenging for fault detection. The results indicate that as the parallel resistance decreases, the impedance spectrum undergoes more significant and systematic changes across the frequency range from 10 kHz to 1 MHz. Fig. 4 provides a zoomed view of this critical frequency band. Fig. 3 demonstrates that at frequencies above 1 MHz, the impedance remains consistent across different R_v values. Based on the theory of high-frequency modeling of electrical machines, impedance exhibits different frequency response characteristics during the switching process during machine operation. Therefore, it can be inferred that the frequency response characteristics from 10 kHz to 1 MHz could be utilized to identify internal short-circuit faults within one phase. This hypothesis is further validated through experimental analysis in the following section.

III. Validation and Analysis Based on Time-Domain Measurement

It is hypothesized that internal short-circuit faults can be detected through the transient behavior of terminal electrical signals. In order to validate this hypothesis, an experiment based on time-domain measurements has been designed. Figures 5 and 6 illustrate the measurement setup. The DFIM stator winding phases U, V, and W are interconnected. The variable resistor R_v is shorted between the U terminal and the neutral point to simulate internal short-circuit faults within one phase. A high-voltage impulse generator equipped with Silicon Carbide (SiC) power modules is used to inject PWM-form voltage between the U terminal and the machine housing. The voltage signal serves as the input signal with a switching

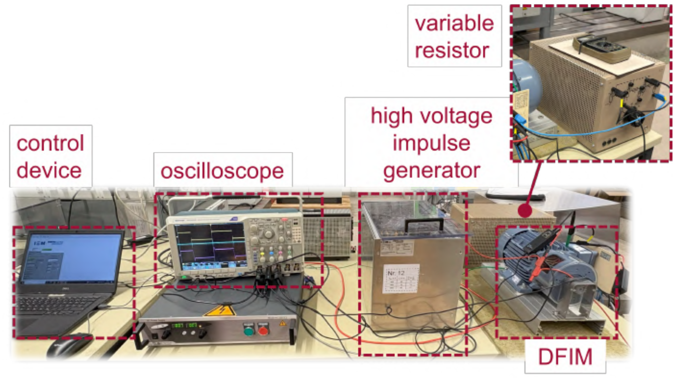

Fig. 5. Test bench for measuring voltage signals at terminals and the neutral point during short-circuiting U-phase winding of the DFIM using variant resistance.

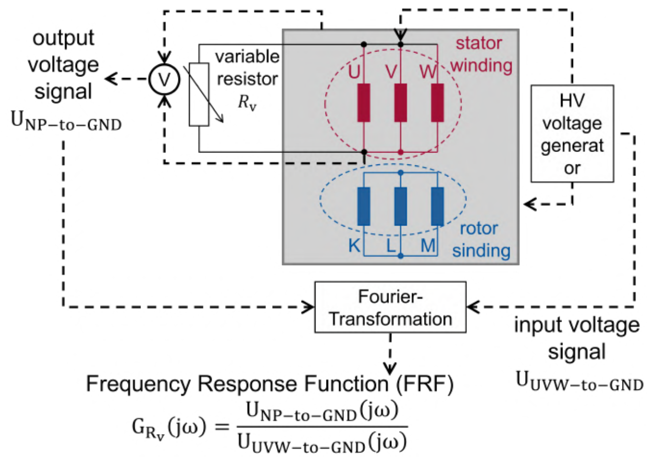

Fig. 6. Diagram for calculating the transmittance transfer function between the terminal and neutral point voltage signals.

frequency f_{sw} of 2 kHz and a DC-link voltage value of 200 V. To detect the internal short circuit in the phase winding, the voltage $U_{NP-to-GND}$ between the neutral point and the machine housing is measured and recorded as the output.

Fig. 7 presents the measurement results. Under the identical excitation voltage $U_{UVW-to-GND}$, the output voltage signal $U_{NP-to-GND}$ shows a noticeable change during switching processes as R_v decreases. The oscillation frequency of $U_{NP-to-GND}$ significantly increases as R_v decreases. Notably, about 0.02 ms after the start of the PWM switching, the oscillatory behavior of the $U_{NP-to-GND}$ signals under different conditions tends to converge to a steady state. It indicates that identifying internal short-circuit faults within one phase is possible by analyzing the transient behavior of terminal voltages during the switching processes.

Previous studies suggest that during analyzing transient voltage signals, the system can be modeled as a Linear Time-Invariant (LTI) system [14]. In order to assess the insulation properties of the machine windings under different R_v values, a Frequency Response Function (FRF), $G_{R_v}(j\omega)$, derived from Fourier Transform techniques, is introduced:

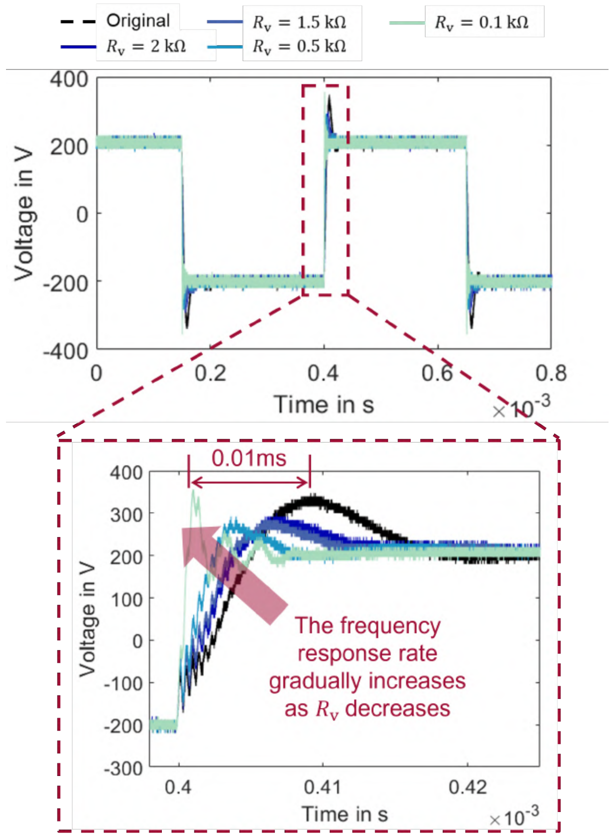

Fig. 7. Comparison between voltage signals $U_{\mathrm{NP-to-GND}}$ at the neutral point for variant R_{v} values.

$$X(\mathrm{j}\omega) = \int_{-\infty}^{\infty} x(t) \cdot e^{-\mathrm{j}\omega t}\, dt \tag{1}$$

$$G_{R_{\mathrm{v}}}(\mathrm{j}\omega) = \frac{U_{\text{NP-to-GND}}(\mathrm{j}\omega)}{U_{\text{UVW-to-GND}}(\mathrm{j}\omega)} \tag{2}$$

where $X(\mathrm{j}\omega)$ in (1) is the Fourier Transform of a time-domain signal $x(t)$. The high-voltage impulse generator used in the experiment generates the excitation voltage signal $U_{\text{UVW-to-GND}}(t)$ with a slew rate of $10\,\mathrm{V\,ns^{-1}}$, which is significantly higher than the rise rate of the resulting voltage signal $U_{\text{NP-to-GND}}(t)$. Based on the FRF defined in (2), $U_{\text{NP-to-GND}}(t)$ is chosen as the corresponding impulse response for analysis. Fig. 8 shows the evaluation of the resulting voltage signal $U_{\text{NP-to-GND}}(t)$. Concerning the steady-state behavior, the settling time t_{Set} and the voltage rise time Δt are calculated for each experimental condition. The statistical results are shown in Fig. 9. With a decrease in R_{v}, corresponding to an expansion of the winding area affected by the short circuit, the settling time t_{Set} decreases, as shown in Fig. 9a. The reason is that the time constant is proportional to the resistance. With lower short-circuited resistance, the oscillation process is, therefore, quicker. At the same time, the rise time Δt decreases with the decreasing R_{v} value, as presented in Fig. 9b, which can also be explained using the explanation of the decreased time constant

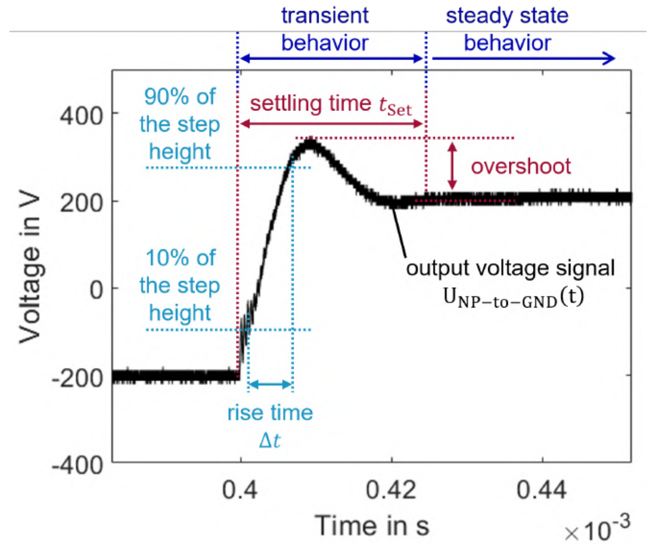

Fig. 8. Characteristic values in the transient voltage signal $U_{\text{NP-to-GND}}(t)$ for further analysis.

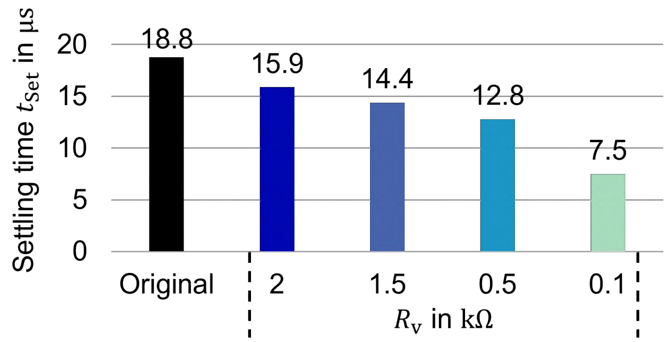

(a)

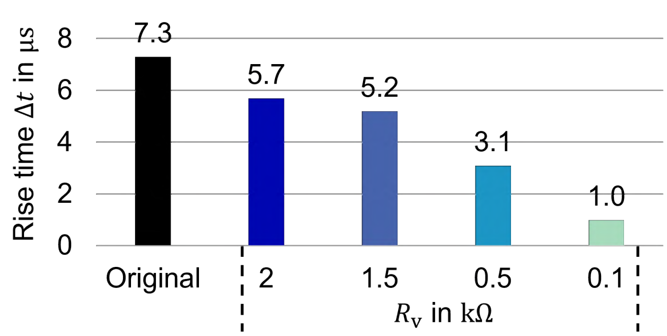

(b)

Fig. 9. Decreased time values observed in the transient voltage signal $U_{\text{NP-to-GND}}(t)$ with decreased short-circuiting resistance: (a) Settling time, (b) Rise time.

due to decreased short-circuited resistance. For further study of the winding behavior under various conditions of R_v, the FRF $G_{R_\mathrm{v}}(\mathrm{j}\omega)$ is analyzed in the time domain.

In this measurement, the oscilloscope's sampling rate is 1.25 GHz, which is far higher than the upper frequency of 10 MHz during the impedance measurement in Section II. In practical signal processing, the continuous Fourier Transform described in (2) can be directly replaced by the Fast Fourier Transform (FFT). After the Fourier Transform, it is followed by denoising and smoothing processes to obtain the spectrum of $G_{R_\mathrm{v}}(\mathrm{j}\omega)$ from 2 kHz to 10 MHz.

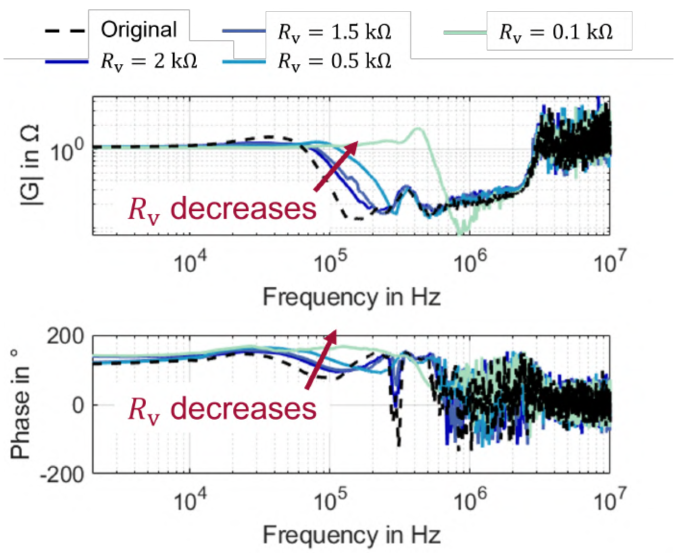

Fig. 10. Bode diagram of $G_{R_\mathrm{v}}(\mathrm{j}\omega)$ varying obviously with decreasing R_v values.

The transfer function $G_{R_\mathrm{v}}(\mathrm{j}\omega)$ und various parallel resistance values R_v is displayed in Fig. 10. It is observed that the changes in $G_{R_\mathrm{v}}(\mathrm{j}\omega)$ are significant enough to reflect the influence from the parallel resistance R_v, compared to the original winding status without a parallel resistance R_v. Due to the sampling accuracy and noise interference during measurement, the frequency spectrum above 3 MHz exhibits severe oscillations and cannot be used for fault detection. Notably, the frequency range over which $G_{R_\mathrm{v}}(\mathrm{j}\omega)$ changes is consistent with the frequency domain segment where the common-mode impedance changes, as discussed in Section II, which further validates the feasibility of using transient signals for online detection of inter-turn short-circuit faults. In order to quantitatively evaluate the influence of parallel resistance R_v on the spectrum of the transfer function $G_{R_\mathrm{v}}(\mathrm{j}\omega)$, the Power Spectral Density $\boldsymbol{PDS}(f)$ is applied, as defined with (3). It represents how the output signal responds to the input signal across various frequency components and the distribution of the system's output signal in terms of power:

$$PSD(f_k) = \left|G_{R_\mathrm{v}}(\mathrm{j}\cdot 2\pi \cdot f_k)\right|^2 \tag{3}$$

Where $f_k = n \cdot f_\mathrm{sw}$ is the integer multiple of the switching frequency f_sw with $n \in \mathbb{Z}^+$. The Pearson Correlation Coefficient ρ_{R_v} under different R_v values is calculated based on the distribution of corresponding short-circuited winding with $\boldsymbol{PDS}_{\mathrm{R_v}} = \{PSD_{R_\mathrm{v}}(f_1), PSD_{R_\mathrm{v}}(f_2), ..., PSD_{R_\mathrm{v}}(f_n)\}$ and the $\boldsymbol{PDS}_\mathrm{org} = \{PSD_\mathrm{org}(f_1), PSD_\mathrm{org}(f_2), ..., PSDR_\mathrm{org}(f_n)\}$ of the original winding without short circuit:

$$\rho_{R_\mathrm{v}} = \frac{\mathrm{cov}(\boldsymbol{PDS}_\mathrm{org}, \boldsymbol{PDS}_{R_\mathrm{v}})}{\sigma_{\boldsymbol{PDS}_\mathrm{org}} \cdot \sigma_{\boldsymbol{PDS}_{R_\mathrm{v}}}} \tag{4}$$

Where:

- $\mathrm{cov}(\boldsymbol{PDS}_\mathrm{org}, \boldsymbol{PDS}_{R_\mathrm{v}})$ is the covariance between $\boldsymbol{PDS}_\mathrm{R_V}$ and $\boldsymbol{PDS}_\mathrm{org}$ from 2 kHz to 3 MHz.
- $\sigma_{\boldsymbol{PDS}_\mathrm{org}}$ and $\sigma_{\boldsymbol{PDS}_{R_\mathrm{v}}}$ are the standard deviations of $\boldsymbol{PDS}_\mathrm{org}$ and $\boldsymbol{PDS}_\mathrm{R_V}$, respectively.

The correlation coefficient ρ_{R_v} ranges between -1 and 1. A value close to 1 indicates a high power spectral density distribution similarity between the two transfer functions. A value closer to 0 suggests a higher deviation from the characteristics of the healthy condition. This way, the correlation coefficient based on $\boldsymbol{PDS}$ compares the fault and healthy cases and indicates the inter-turn short circuit.

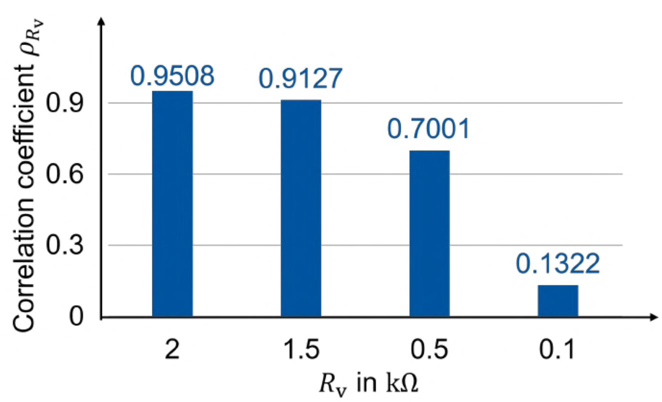

Fig. 11. Calculated ρ_{R_v} for short-circuit cases with variant R_v, whereby the original stator winding without short circuit is used as reference.

Fig. 11 shows the correlation coefficient ρ_{R_v} at various resistance values R_v across the frequency range of 2 kHz to 3 MHz. When a resistor of 1.5 kΩ is connected in parallel with the U-phase winding, the ρ_{R_v} decreases to about 0.9. It indicates that the changes in the correlation coefficient are sensitive to internal short circuits within one phase. Furthermore, such changes are also observed by comparing the transient signals of the terminal voltage in the time domain, as shown in Fig. 7. As the parallel resistance value decreases further, the correlation coefficient undergoes more noticeable changes, consistent with the variations observed in the common-mode impedance in Fig. 3 and the time-domain signals in Fig. 7.

As previously mentioned, different values represent the location and severity of internal short-circuit faults in the winding. Based on the analysis, it is sufficient to demonstrate that internal insulation faults in electrical machines can be quickly identified by capturing and analyzing the transient behavior of machine terminal voltage signals. It is important to note that the electric machines used in industry—such as wind power generators, marine engines, and large mining motors—are significantly larger than the DFIM stator winding discussed in this paper. The increased size of these machines tends to reduce the oscillation frequency of transient behaviors in generator terminal voltage signals. Consequently, this lowers the necessary sampling frequency to several hundred kilohertz, rather than the gigahertz levels required when using an oscilloscope.

IV. Conclusions and Outlooks

This study has successfully validated an innovative online method for identifying internal insulation faults in electrical machines. This method effectively detects such faults by analyzing the transient behaviors of terminal voltage signals. Compared to partial discharge-based online detection, it is less sensitive against the background of the electrical machines. Moving forward, we will further confirm its applicability to real electric machines by analyzing actual operating environments. For example, the inter-turn short circuit fault will be carried out precisely between the adjacent winding of the same phase instead of using a resistance between the phase terminal and the neutral point. The method's sensitivity against the inter-turn short circuit fault at different operational temperatures will also be evaluated. Another research point will focus on developing real-time online monitoring algorithms based on this approach.

References

[1] M. Rausand and A. Hoyland, *System reliability theory: models, statistical methods, and applications*. John Wiley & Sons, 2003, vol. 396.

[2] F. K. Moghadam and A. R. Nejad, "Online condition monitoring of floating wind turbines drivetrain by means of digital twin," *Mechanical Systems and Signal Processing*, vol. 162, p. 108087, 2022.

[3] Siemens AG, "SIPLUS CMS1200 - Digital Drive Train Connectivity," 2025, accessed January 18, 2025. [Online]. Available: https://www.siemens.com/de/de/produkte/antriebstechnik/digitaler-antriebsstrang/konnektieren/siplus-cms1200.html

[4] Bachmann Electronic GmbH, "CMSadvanced - Condition Monitoring System," 2025, accessed January 18, 2025. [Online]. Available: https://www.bachmann.info/en/products/cmsadvanced

[5] G. C. Stone, I. Culbert, E. A. Boulter, and H. Dhirani, *Electrical insulation for rotating machines: design, evaluation, aging, testing, and repair*. John Wiley & Sons, 2014.

[6] J. Leffler and P. Trnka, "Failures of electrical machines-review," in *2022 8th International Youth Conference on Energy (IYCE)*. IEEE, 2022, pp. 1–4.

[7] Y. He, M. Jiang, K. Sun, M. Qiu, and D. Gerada, "Analysis on rotor vibration characteristics under dynamic rotor interturn short circuit fault in synchronous generators," *Energies*, vol. 16, no. 18, p. 6585, 2023.

[8] T. N. Santelo, C. M. R. de Oliveira, C. D. Maciel, and J. R. B. de A. Monteiro, "Wind turbine failures review and trends," *Journal of Control, Automation and Electrical Systems*, pp. 1–17, 2022.

[9] J. d. S. Cruz, F. Fruett, R. d. R. Lopes, F. L. Takaki, C. d. A. Tambascia, E. R. d. Lima, and M. Giesbrecht, "Partial discharges monitoring for electric machines diagnosis: A review," *Energies*, vol. 15, no. 21, 2022. [Online]. Available: https://www.mdpi.com/1996-1073/15/21/7966

[10] G. C. Montanari and R. Ghosh, "Wind farm electrical asset components: Insulation diagnostics through partial discharge measurements," in *2021 IEEE Green Technologies Conference (GreenTech)*, 2021, pp. 586–592.

[11] J. Ortego, E. Arcones, C. Vera, F. Álvarez, F. Garnacho, and A. Khamlichi, "Processing techniques applied to partial discharge measuring in rotating machines," in *2020 IEEE 3rd International Conference on Dielectrics (ICD)*, 2020, pp. 898–901.

[12] D. A. Hewitt, S. Sundeep, J. Wang, and A. Griffo, "High frequency modeling of electric machines using finite element analysis derived data," *IEEE Transactions on Industrial Electronics*, vol. 71, no. 2, pp. 1432–1442, 2023.

[13] H. Peng, S. Stevic, Z. Luo, N. Driendl, D. Butterweck, L. Sharifian, Y. Firouz, and K. Hameyer, "Voltage distribution modeling along stator windings in permanent magnet synchronous machines using coil-based grey box models," *IEEE Transactions on Energy Conversion*, 2024.

[14] H. Peng, Z. Luo, Y. Yu, and K. Hameyer, "Modeling voltage distribution along the hairpin windings of an electrical machine using impedance fitting," in *2024 International Conference on Electrical Machines (ICEM)*. IEEE, 2024, pp. 1–7.

[15] Y. Norouzi, C. Frohne, and P. Werle, "High frequency model of cables for frequency domain analysis used for fault localization," in *2018 IEEE International Conference on High Voltage Engineering and Application (ICHVE)*. IEEE, 2018, pp. 1–4.

[16] L. Ranzinger, S. Uhrig, and S. Tenbohlen, "Analysis and modeling the frequency response of rotating machines regarding fault diagnosis using sfra," *IEEE Transactions on Energy Conversion*, vol. 39, no. 1, pp. 747–756, 2023.

[17] C.-N. Behrendt, J. Dittmann, and B. Ponick, "Sensitivity of the common-mode characteristics of a stator winding regarding the assumed hairpin position in a slot," in *IECON 2023-49th Annual Conference of the IEEE Industrial Electronics Society*. IEEE, 2023, pp. 1–6.

[18] M. Diab, W. Zhou, C. Emersic, X. Yuan, and I. Cotton, "Impact of pwm voltage waveforms on magnet wire insulation partial discharge in sic-based motor drives," *IEEE Access*, vol. 9, pp. 156 599–156 612, 2021.

[19] F. Alvarez-Gonzalez, D. Hewitt, A. Griffo, and J. Wang, "Challenges of common mode current and voltage acquisition for stator winding insulation health monitoring," in *2020 IEEE Energy Conversion Congress and Exposition (ECCE)*. IEEE, 2020, pp. 4452–4459.

[20] M. Saeed, D. Fernández, J. M. Guerrero, I. Díaz, and F. Briz, "Insulation condition assessment in inverter-fed motors using the high-frequency common mode current: A case study," *Energies*, vol. 17, no. 2, p. 470, 2024.

[21] Keysight Technologies, "E4990A Impedance Analyzer (20 Hz - 10, 20, 30, 50, 120 MHz)," 2025, accessed: Jan. 18, 2025. [Online]. Available: https://www.keysight.com/de/de/product/E4990A/impedance-analyzer-20-hz-10-20-30-50-120-mhz.html

[22] A. U. Rehman, W. Jiao, J. Sun, M. Sohaib, Y. Jiang, M. Shahzadi, and M. I. Khan, "Efficient fault detection of rotor minor inter-turn short circuit in induction machines using wavelet transform and empirical mode decomposition," *Sensors*, vol. 23, no. 16, p. 7109, 2023.